

Effect of Broaching Machining Parameters on Low Cycle Fatigue Life of Ni-Based Powder Metallurgy Superalloy at 650 °C

ZHANG Lu^{1,2}, LI Weilong^{1,2}, WANG Yuzhuo^{1,2},
YU Zhiwei^{1,2}, JIANG Rong^{1,2}, SONG Yingdong^{1,2,3*}

1. Key Laboratory of Aero-engine Thermal Environment and Structure, Ministry of Industry and Information Technology, College of Energy and Power Engineering, Nanjing University of Aeronautics and Astronautics, Nanjing 210016, P.R. China;
2. Jiangsu Province Key Laboratory of Aerospace Power System, College of Energy and Power Engineering, Nanjing University of Aeronautics and Astronautics, Nanjing 210016, P.R. China;
3. State Key Laboratory of Mechanics and Control Mechanical Structures, Nanjing University of Aeronautics and Astronautics, Nanjing 210016, P.R. China

(Received 23 May 2023; revised 14 September 2023; accepted 23 October 2023)

Abstract: Effects of different broaching machining techniques on fatigue damages are studied. Low cycle fatigue tests at high temperature 650 °C in air environment are carried out for specimens with four processing techniques. The roughness characterization method, electron backscatter diffraction (EBSD) and nanoindentation test are used to obtain the surface roughness, residual stress and work hardening, respectively. The wire cut electrical discharge machining (WEDM) specimens exhibit the highest fatigue life of average 80 360 cycle with the lowest surface roughness of 0.226 and residual stress, while specimens machined by blunt tool suffer the lowest fatigue life of average 43 978 cycle, decreasing 45% compared to WEDM ones. SEM results show that fatigue cracks are mainly initiated from the coarse non-recrystallized grains and machining defects. The broaching machining methods and parameters have significant influences on the level of fatigue damages and fatigue lives.

Key words: broaching machining techniques; fatigue life; nickel-based powder metallurgy superalloy; surface roughness; residual stress; work hardening

CLC number: V216.3 **Document code:** A **Article ID:** 1005-1120(2023)05-0511-11

0 Introduction

Nickel-based powder metallurgy superalloy is a kind of metal material suitable for aeroengines, but it is also vulnerable to the influence of machining process on fatigue life. The damage generated in the machining process will cause the fatigue damage to the high load components, thus damaging the integrity of components^[1-2].

The failure of surface integrity is the main inducement of fatigue failure^[3-4]. Machining damage will lead to surface tearing, inclusion cracking, cavity formation, carbide cracking or grain pulling,

which will undermine the surface integrity of parts^[1,5-8]. Aggressive machining conditions will produce a “white layer” composed of nanoscale grain structure to induce local changes in the microstructure^[5-9]. Under high temperature and high stress conditions, such changes will seriously reduce the fatigue life^[1,9-10]. In addition, local stress concentration during machining will also lead to early crack initiation^[11-12]. Quan et al.^[13] used the stress concentration factor to measure the fatigue life, and the results showed that the emergency concentration factor and the fatigue life fitted well.

*Corresponding author, E-mail address: ydsong@nuaa.edu.cn.

How to cite this article: ZHANG Lu, LI Weilong, WANG Yuzhuo, et al. Effect of broaching machining parameters on low cycle fatigue life of Ni-based powder metallurgy superalloy at 650 °C[J]. Transactions of Nanjing University of Aeronautics and Astronautics, 2023, 40(5): 511-521.

<http://dx.doi.org/10.16356/j.1005-1120.2023.05.001>

The fatigue life of turbine components is very important to the integrity of aeroengines when they work under high temperature and high load. The turbine components are usually manufactured by broaching. Since turbines are usually made of high strength super-alloy materials, the increased cutting rates and feed rates will lead to an increase in the degree of work hardening of the “white layer”^[14-15]. Meanwhile, broaching tools will have rapid wear^[16], which is affected by broaching speed, broaching force, lubrication and other factors^[12,17]. Tool wear can lead to changes in coating and surface roughness^[1,18], and the inevitable vibration in the machining process will also lead to the increase of surface roughness^[19], and ultimately affect the fatigue life. Rengen et al.^[20] studied the surface integrity characteristics of Udimet 720Li under slight damage and damage machining conditions. The correlation between machining conditions and plastic deformation is established. The mechanical effect of traditional machining can lead to serious plastic deformation and work hardening of metal workpiece^[2]. Therefore, the hardness characterization of specimens in fatigue test is indispensable. The residual stress produced by machining will also affect the fatigue life^[21-23], and the dominant factor is to consider the equivalent stress of shear stress and normal stress at the same time^[24-25].

There is little research on the effect of machining conditions on the fatigue life of nickel base superalloys. Quan et al.^[26] conducted a comparative study on the surface integrity and fatigue performance of GH4169 superalloy components manufactured by the combined process of milling, grinding and polishing. The results show that polishing has the greatest influence on fatigue performance, and a typical “hook” residual stress distribution is produced on the surface by milling. Chen et al.^[27] studied broaching operations (similar to the machining of cold wood grooves on turbine disks) and the subsequent heat treatments at 550 °C and 650 °C on fatigue properties and corresponding crack initiation behavior. The combined effect of heat treatment on the fatigue properties and corresponding crack initiation behavior of forged Inconel 718. The research shows that the broaching specimen has a longer fatigue life than

the polished one, but the 650 °C-heat treatment reduces the fatigue life of the broaching specimen and increases the fatigue life of the polished specimen. Telesman et al.^[28] studied the influence of tool wear and broaching speed on fatigue life. The research shows that the average fatigue life of “blunt” cutter is longer, but the fatigue life is more dispersed at different broaching speeds. Connolley et al.^[29] studied the influence of different broaching processes on fatigue life at 600 °C. The research shows that fatigue life is related to surface roughness, and notch polishing has a favorable effect on fatigue life.

In this paper, the influence of different machining conditions on the fatigue life of the third-generation nickel base powder superalloy is studied. The surface roughness, hardness and electron backscatter diffraction (EBSD) characterization of specimens with different machining conditions are carried out, and the influence of different machining conditions on the fatigue life and fracture characteristics are analyzed.

1 Materials and Methods

1.1 Material and specimen machining

The third-generation nickel-based powder metallurgy superalloys is used in this study. The specimen is designed according to the standard GB/T 3075—2008 as shown in Fig. 1. Specimens are 95 mm in length. Middle segment of specimen is 11 mm in width and 3 mm in thickness. M4×23 threads are machined in both ends of specimen to suit the fixture. Connections between the threaded specimen and the middle specimen are chamfered to reduce the stress concentration. A finite element model with a notch r of 4 mm, depth of 1.3 mm, the elastic modulus of 169 GPa at 650 °C and Poisson’s ratio of 0.3 is established. The fixed constraint is applied to the right end face with the triangular waveform with stress ratio of 0.05, the maximum stress of 700 MPa and frequency of 10 Hz. The results show that the maximum stress and maximum strain are both at root of the notch, with the value of 1 413 MPa and 0.823%, respectively. The location and depth of the notch can be therefore determined. The notch with radius r of 4 mm and depth of 1.3 mm is processed in the middle of specimens.

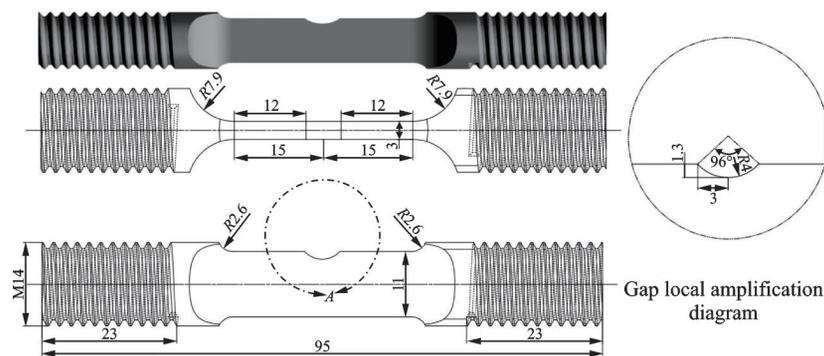


Fig.1 Specimen shape and dimension drawing and some processed test pieces (Unit: mm)

Through repeated trial production and exploration of different machining techniques (wire-electrode cutting, conventional tool and blunt tool) and machining parameters (milling spindle speed and feed rate), the roughness and other indicators caused by machining are investigated, and the following four machining conditions are finally determined. (1) Wire cut electrical discharge machining

(WEDM), slow-feeding EDM wire-cut + removal of surface corrosion layer; (2) conventional tool, feed rate F260, spindle speed S2800; (3) conventional tool, feed rate F260, spindle speed S2000; (4) blunt tool, feed rate F600, spindle speed S3500. Five sets of experiments are performed for each process condition as shown in Table 1.

Table 1 Experimental scheme for research on effect of machining damage on fatigue properties of powder superalloys

Machining technology	Machining parameter	
WEDM	Slow-feeding EDM wire-cut + Removal of surface corrosion layer	
Conventional tool	Feed rate F260	Spindle speed S2800
	Feed rate F260	Spindle speed S2000
Blunt tool	Feed rate F600	Spindle speed S3500

Under the condition of 650 °C, triangular wave stress with a stress ratio of 0.05 and a frequency of 10 Hz is applied to the test piece for fatigue test. The maximum load applied shall ensure that the maximum strain at the bottom of the notch is 0.823%.

1.2 Fatigue test and fracture analysis method

The test is carried out by a 100 kN MTS Landmark hydraulic-servo fatigue testing machine combined with a high temperature furnace. The test system consists of heating, loading, cooling, temperature monitoring and other parts. The fatigue testing machine is used for loading, and the high temperature furnace is used for heating with one thermocouple, connected to temperature monitoring. The fatigue test equipment is shown in Fig.2. Fatigue life is obtained by repeated stretching until specimen failure. The fatigue test is stress-controlled, with the

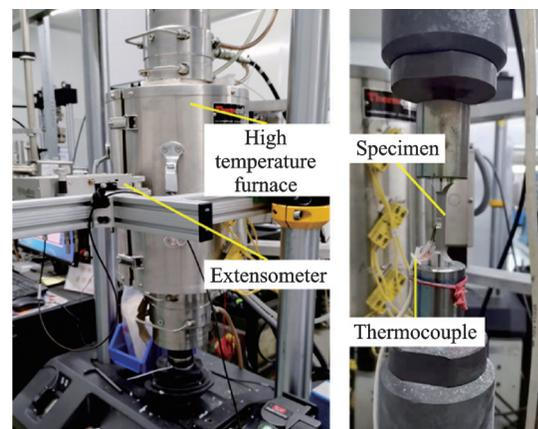


Fig.2 Low cycle fatigue test equipment

maximum stress of 700 MPa, stress ratio of 0.05 and frequency of 10 Hz, at temperature of 650 °C.

In order to reveal the damage mechanism of the material under uniaxial thermomechanical fatigue load, after the fatigue failure, the fracture is cut off and cleaned with an ultrasonic cleaner. When fracture occurs, the acceleration voltage is set to 15 kV.

1.3 Specimen characterization method

The notch roughness under different machining technologies is tested by Taylor Hobson Form Taly-surf i-Series 5 shape and surface roughness tester. The thimble is in contact with the surface of the notch root, and the trajectory is reciprocated three times to obtain the average value of the measured roughness. Nano Test Vantage is used to measure the microhardness in the notch root area of specimens with different machining techniques. In order to exclude the influence of acquisition parameters on the related data of different specimens, the uniform load for microhardness measurement is 20 mN, the holding time is 30 s, the microhardness indentation spacing is 4 μm , and the area size is 32 $\mu\text{m} \times 48 \mu\text{m}$. In the process of hardness and characterization EBSD analysis of FGH4099 notched specimens under different machining conditions, a 400 $\mu\text{m} \times 400 \mu\text{m}$ area at the root of the notched specimen is selected for observation. It is selected mainly because the load on this area during the specimen machining is relatively high. It can be used to evaluate the residual stress field introduced by different machining processes and the variation law of residual stress on fatigue life during subsequent low-cycle fatigue tests. In order to avoid excessive deformation, the processed notch specimen is cut by EDM machining method, and then 400#, 800#, 1000#, 2000#, 3000# and 5000# sandpapers are used for grinding and polishing in turn by cold inserting treatment. Then, the specimens are mechanically polished with oxide polishing suspension for 20 min, and finally electropolished with 10 ml perchloric acid and 90 ml ethanol solution for 10 s. EBSD measurements are performed on a Zeiss Gemini

500 field emission SEM equipped with an Oxford EBSD detector. In order to exclude the influence of EBSD acquisition parameters on the disorientation data of different specimens, a series of unified parameters, 15 kV accelerating voltage, 60 μm aperture and 0.5 μm step size, are adopted. Finally, the EBSD data are processed using Aztec Crystal software and the open-source toolbox MTEX, and the derived geometrically necessary dislocation (GND) density maps are calculated with a 3×3 core size.

2 Experiment Results

2.1 Influence of machining conditions on fatigue life and fracture analysis

To avoid the influence of randomness on the four machining technologies, five groups of experiments are conducted under each machining technology. The results of fatigue life are given by low cycle fatigue test equipment, represented by the number of cycle when specimen breaks. The average low cycle fatigue life and average notch roughness under four processes are compared as shown in Fig.3. The average fatigue life of specimens machined by WEDM is the highest with 80 360 cycle, and that of specimens machined by blunt tool is the lowest with 43 978 cycle. The average fatigue life of specimens machined by conventional tool decreases from 72 035 to 48 603 when spindle speed decreases from 2 800 r/min to 2 000 r/min. It is observed that the average low cycle fatigue life is negatively correlated with the average notch roughness. That is, the higher the roughness, the shorter the life, but not linearly correlated. It is observed that the average roughness of notch is less than or equal to 0.8 μm and the average low cycle fatigue life decreases gradually with the increase of roughness in the range of

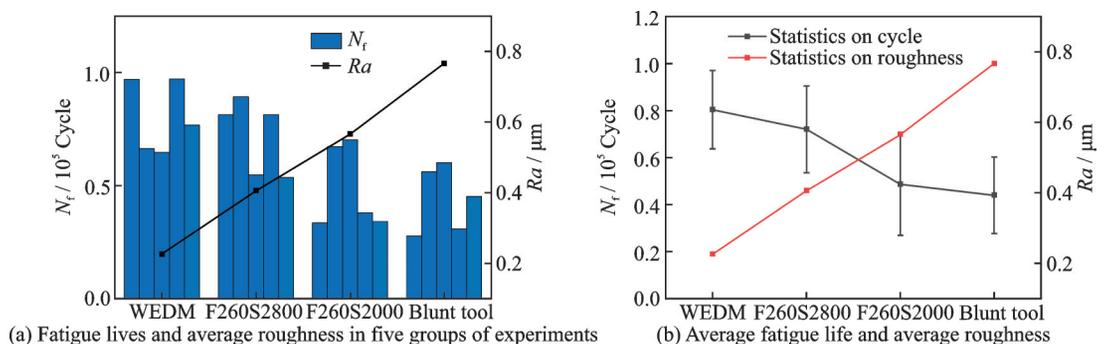


Fig.3 Relationship between average low cycle fatigue life and average notch roughness in different machining processes

$0.6 \times 10^5 - 1.0 \times 10^5$. While the average notch roughness is greater than $0.8 \mu\text{m}$, the average low cycle fatigue life is about 0.6×10^4 .

For each machining technology, a typical fatigue fracture is selected for SEM characterization. The microstructures of the fatigue fracture surfaces of the specimen machined by WEDM and surface corrosion layer removal machining technology are shown in Fig.4. Under this machining technology, the cracks of specimen are initiated from the coarse non-recrystallized grains on the sub surface at the

center of the notch root, and these cracks exhibit transgranular propagation^[30-32]. Fatigue bands and secondary cracks exhibiting transgranular propagation can be observed in the crack growth area, and there are a lot of step slip surfaces similar to cleavage in the transient fault zone. It shows that due to the minimum notch work hardening and the minimum plastic deformation under this machining technology, the cracks are initiated from the material defects inside the specimen, and this case has the longest average low-cycle fatigue life.

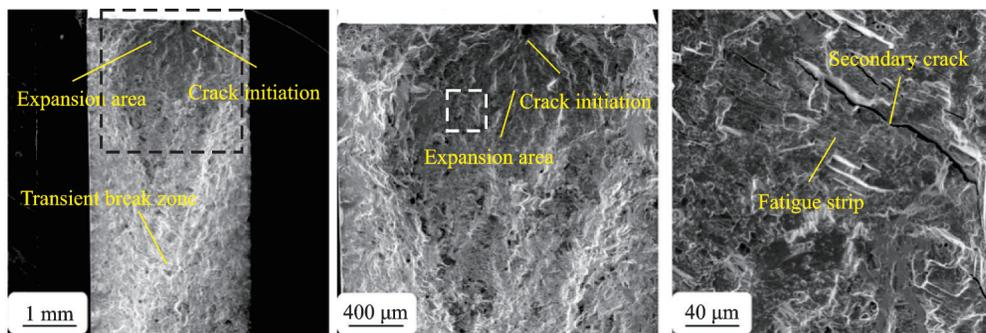


Fig.4 Low cycle fatigue micro fracture diagram of WEDM specimen

The microstructure of the fatigue fracture surface of the specimen machined by conventional tool with F260S2800 is similar to that of WEDM, as shown in Fig.5. Under this machining technology, the cracks of specimen are also initiated from the non-recrystallized grains on the sub surface at the right of the notch root, and the cracks exhibit trans-

granular propagation. The fatigue bands and secondary cracks exhibiting transgranular propagation can be observed in the crack propagation area, and secondary cracks can be observed in the transient fracture area. The cracks are initiated from the material defects on the sub-surface of the specimen under this machining condition.

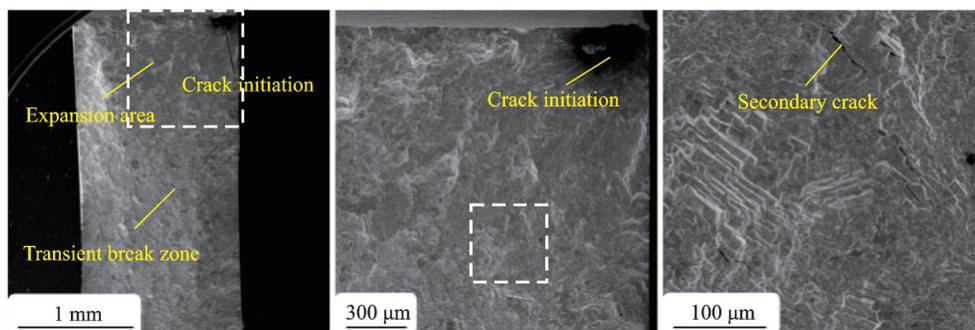


Fig.5 Low cycle fatigue micro fracture diagram of F260S2800 specimen

The microstructure of the fatigue fracture surface of the specimen machined by conventional tool with F260S2000 is similar to that of WEDM, as shown in Fig.6. Under this machining technology, the cracks of specimen are initiated at the left edge of the notch root at the machining defect location. Due

to the machining defects, the stress concentration between the notch root surface and the side interface has led to the initiation of cracks at the left edge of the notch root section. The crack exhibits transgranular propagation, and a secondary crack can be observed in the crack transient zone. Compared with the con-

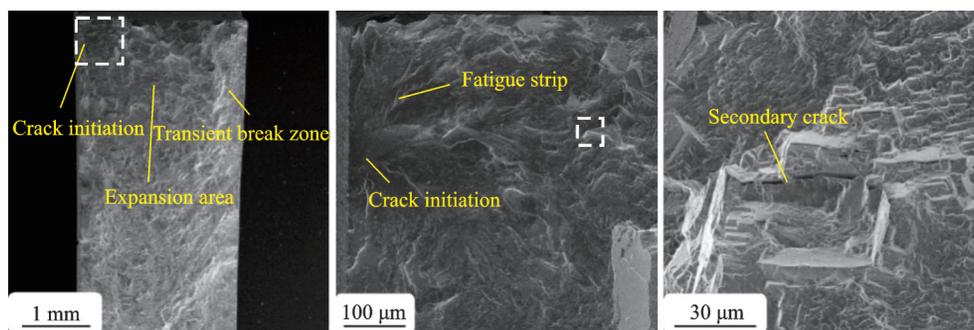


Fig.6 Low cycle fatigue micro fracture diagram of F260S2000 specimen

ventional tool with F260S2800, this kind of machining condition brings higher work hardening and plastic deformation due to greater roughness. Therefore, the crack is initiated from the machining defects at the corner of the notch root, resulting in a significant reduction in the average low cycle fatigue life.

The microstructure of fatigue fracture surface of the specimen machined by blunt tool with F600S3500 machining technology is similar to that of WEDM, as shown in Fig. 7. Under this machining technology, the crack source of specimen is at the left edge of the notch root where there is a machining defect. Because of the machining defect, the stress at the inter-

face between the notch root surface and the side surface is concentrated, which leads to the crack initiation at the upper left corner of the notch root cross section. The crack propagates transgranularly. Fatigue striations are observed in the crack growth zone, and there is a step like sliding surface similar to cleavage in the transient fracture zone. Blunt tools produce large plastic deformation, so cracks are initiated from the machining defects where the surface of the notch root meets the flank. The average low cycle fatigue life under this machining condition is the smallest but not much different from the average low cycle fatigue life of the conventional tool with F260S2000.

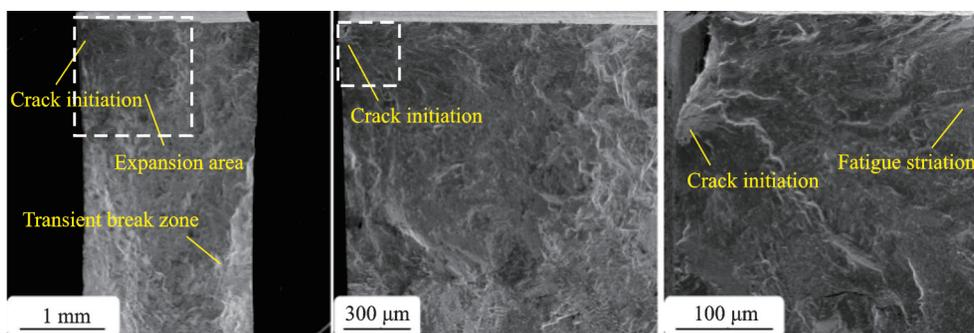


Fig.7 Low cycle fatigue micro fracture diagram of blunt tool specimen

2.2 Roughness characterization results

Roughness test is carried out on the notches

processed by four different processes, whose results are shown in Table 2.

Table 2 Test results of notch roughness of different machining processes

Machining processes		Roughness	Benchmarking roughness
Machining technology	Machining parameters		
WEDM	Slow-feeding EDM wire-cut +	0.226	0.2
	Removal of surface corrosion layer		
Conventional tool	Feed rate F260 Spindle speed S2800	0.406	0.4
	Feed rate F260 Spindle speed S2000	0.566	0.6
Blunt tool	Feed rate F600 Spindle speed S3500	0.776	0.8

Among the four machining conditions, slow-feeding EDM wire-cut has the lowest surface roughness, and blunt tool milling with a feed rate of F600 and a spindle speed of S3500 has the highest surface roughness. Higher spindle speeds for conventional tool milling correspond to lower surface roughness.

2.3 EBSD microstructure characterization results and hardness characterization

EBSD characterization results of four machining notches (WEDM, conventional tool cutting with F260S2800, conventional tool cutting with F260S2000, blunt tool cutting with F600S3500) are shown in Fig.8. There are about six grains in the transverse range, and the presence of strengthening phase can be clearly seen in the EBSD image. It can be seen from the GND image that the specimen machined by blunt tool has the highest geometrically necessary dislocations on the whole. The work hardening layer of WEDM is the thinnest, and the work hardening layer of blunt tool is thicker. With the decrease of rotational speed, the work hardening layer of specimen machined by conventional tool thickens. The effect of machining technology to the working hardening of specimens is obvious. The work hardening of specimens machined by WEDM is the smallest and that of specimens machined by blunt tool is the biggest. With the increase of spindle speed, the work hardening of specimens machined by conventional tool decreases.

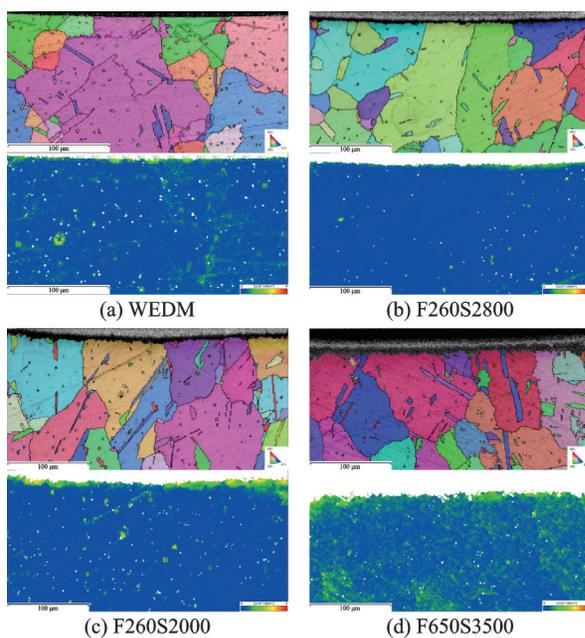


Fig.8 EBSD of four machining notches

In order to qualitatively analyze the plastic deformation caused by work hardening at the notch, the GND value of the notch with smaller roughness in each machining technology is selected for comparison. The GND value of most areas in the visual field is small, and the GND value at the notch is large, so the part with $GND=0.5$ is selected for comparison. The GND distribution of the notch of the four machining processes is shown in Fig.9. It is found that the depth of work hardening under the slow-feeding EDM wire-cut process is the minimum, and the depth of work hardening under the F350S3500 process is the maximum. The peak of GND close to notch root of specimens machined by blunt tool is the biggest at $1.464 \times 10^{14}/m^2$, and that of specimens machined by WEDM is the smallest at $0.985 \times 10^{14}/m^2$. With the spindle speed decreasing from 2 800 r/min to 2 000 r/min, the peak of GND close to notch root of specimens machined by conventional tool increases from 1.065 to 1.330.

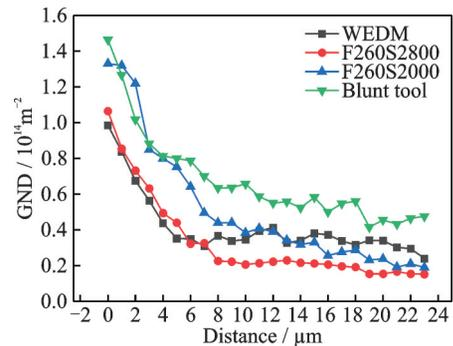


Fig.9 GND distribution diagram of notch in different machining processes

The hardness of $32 \mu m \times 48 \mu m$ area at the notch root of four machining technologies is characterized. The results are shown in Figs.10—12. With the increase of the distance from the notch, the depth of indentation becomes deeper and deeper, indicating that the work hardening decreases with the increase of the distance from the notch, and finally tends to be stable. WEDM and F260S2800 have the lower hardness at the notch root, F260S2000 and Blunt tool has the higher hardness. Blunt tool has the thickest work hardening layer and the work hardening layer of WEDM and F260S2800 is thinner. The hardness of notch root of specimens machined

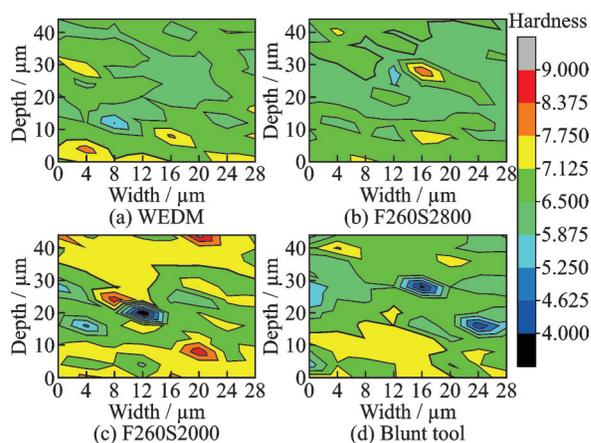


Fig.10 Hardness nephogram of notch root with different machining technologies

by blunt tool is the biggest at 7.507 GPa, and that

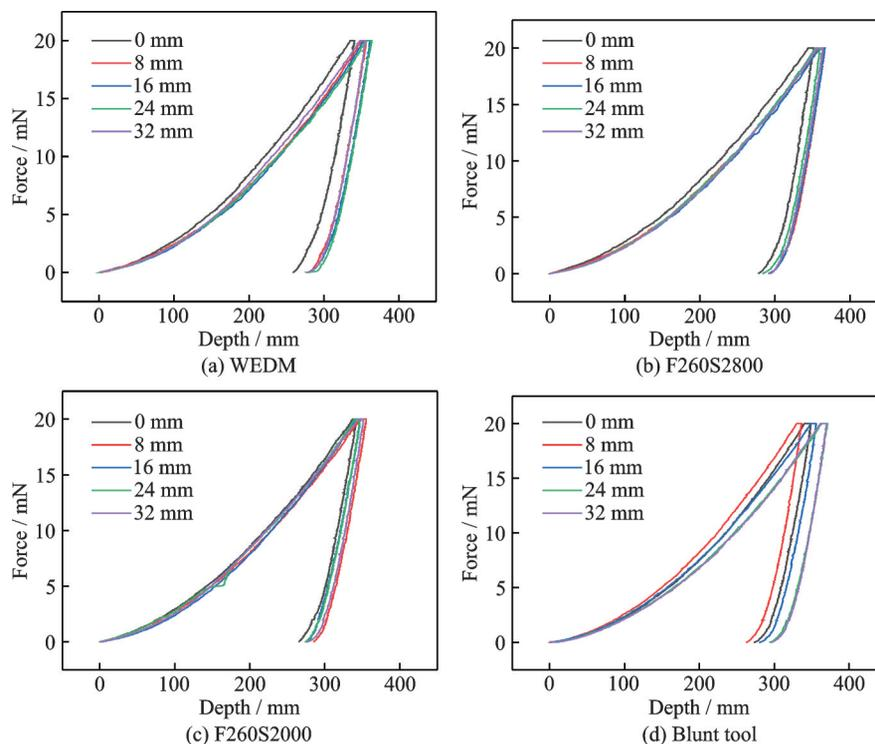


Fig.12 Force-depth curves of nanoindentation tests for different machining technologies

3 Discussion

Specimens machined by blunt tool has the lowest fatigue life, with the highest residual stress and work hardening. Specimens machined by WEDM has the highest fatigue life, with the lowest residual stress and lower work hardening. Effect of spindle speed to specimens machined by conventional tool is obvious, in which the spindle speed increases 800 r/min, the fatigue life increases 48%, and the residual stress and the work hardening decrease. The fatigue damage of WEDM is the smallest, and the

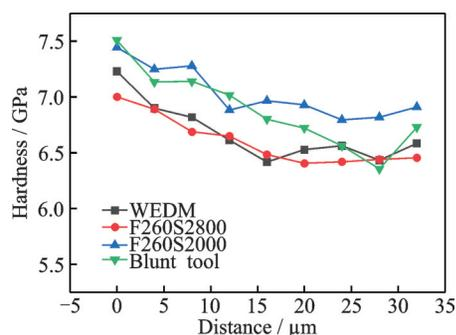


Fig.11 Variation of hardness with notch distance

of specimens machined by conventional tool F260S2800 is the smallest at 7.001 GPa. The work hardening of specimens machined by conventional tool is higher with spindle speed slower.

blunt tool has the worst fatigue damage on specimens.

Through SEM characterization of fractures, it is found that under the two machining parameters of low surface roughness and work hardening, the machining defects are not enough to produce cracks, and the cracks are caused by the internal defects of the material. Under these two machining parameters, the fatigue life of the specimen is higher. However, when the surface roughness and work hardening are higher, the crack initiation occurs at the

stress concentration of the machining defect, so the specimen is more prone to fatigue fracture. The fatigue life is higher when the cracks are initiated from the defects at the subsurface, while the crack initiation at the specimen surface leads to lower fatigue life.

Secondary cracks are caused by weak structures in the plastic zone around the main cracks in the process of material failure, which may be related to metal preparation processes such as inclusion, grain orientation such as large angle grain boundaries and other structures. The fatigue life of the material is mainly affected by the crack initiation mode. In the low cycle fatigue life, the crack initiation life occupies the main part and the crack propagation life is secondary.

The influence of different machining technologies on fatigue life is investigated. As shown in Fig.3, the surface roughness is inversely proportional to the fatigue life. There is no significant difference in the work hardening between F260S2800 and WEDM through EBSD and hardness characterization, indicating that the fatigue failure of these two machining processes is mainly affected by surface roughness. The work hardening degree of F260S2000 and blunt tool is significantly higher than that of WEDM and F260S2800, and the fatigue life of specimens under these two machining techniques is lower. There is little difference in work-hardening between F260S2000 and blunt tool, but there is a big difference in surface roughness. Result shows that there is little difference in fatigue life between F260S2000 and blunt tool, and the influence of roughness on fatigue life is small when the roughness is greater than or equal to $0.563\ \mu\text{m}$. The cracks of specimens machined by blunt tool and conventional tool with F260S2000 are initiated at stress concentration caused by the combination of high surface roughness and work hardening, which gives a shorter fatigue crack initiation time.

According to the analysis of the fracture, the work hardening of WEDM and F260S2800 notch is small, the work hardening of F260S2000 and blunt tool is significantly higher, and the crack initiation is concentrated in the machining defect of notch root.

4 Conclusions

For the third-generation nickel-based superalloy FGH4099, the influence of different machining techniques to the damage of specimens on low-cycle fatigue properties are studied. The conclusions are as follows.

(1) The order of machining techniques with the notch surface roughness increasing from 0.226 to 0.776 is as follows: WEDM, conventional tool with F260S2800, conventional tool with F260S2000, and blunt tool with F600S3500.

(2) WEDM and removal of the surface corrosion layer have the least residual work hardening and minimum plastic deformation. Compared with conventional tool, blunt tool has more work hardening and greater plastic deformation.

(3) The average low cycle fatigue life is negatively correlated with the average notch roughness. That is, the higher the roughness, the shorter the life, but it is not linear. The fatigue life decreases 45% when the surface roughness increases 243%.

(4) The average roughness sum is less than or equal to $0.405\ \mu\text{m}$, and the defect size produced by machining is too small to produce cracks. When the average roughness is greater than or equal to $0.563\ \mu\text{m}$, the low cycle fatigue life is mainly affected by the notch machining defects. The notch roughness is large, and the crack starts from the stress concentration of machining defect at the notch root.

(5) The level of fatigue damage of specimens machined by WEDM is the lowest with the highest fatigue life of 80 360 cycle, and specimens machined by blunt tool suffer the most significant fatigue damage with the lowest fatigue life of 43 978 cycle.

References

- [1] M' SAOUBI R, OUTEIRO J C, CHANDRASEKHARAN H, et al. A review of surface integrity in machining and its impact on functional performance and life of machined products[J]. *International Journal of Sustainable Manufacturing*, 2008, 1(1/2): 203-236.
- [2] LIAO Z R, LA MONACA A, MURRAY J, et al. Surface integrity in metal machining—Part I, Fundamentals of surface characteristics and formation mechanisms[J]. *International Journal of Machine Tools and Manufacture*, 2021, 162: 103687.
- [3] MADARIAGA A, GARAY A, ESNAOLA J A, et

- al. Effect of surface integrity generated by machining on isothermal low cycle fatigue performance of Inconel 718[J]. *Engineering Failure Analysis*, 2022, 137: 106422.
- [4] MARTIN-MEIZOSO A, MARTINEZ-ESNAOLA J M, ARRAZOLA P J, et al. Surface machining condition and fatigue life on Inconel 718[J]. *Procedia Structural Integrity*, 2018, 13: 1609-1614.
- [5] SHARMAN A R C, HUGHES J I, RIDGWAY K. An analysis of the residual stresses generated in Inconel 718TM when turning[J]. *Mater Process Technol*, 2006, 173(3): 359-367.
- [6] CHAMANFAR A, MONAJATI H, ROSENBAUM A, et al. Microstructure and mechanical properties of surface and subsurface layers in broached and shot-peened Inconel-718 gas turbine disc fir-trees[J]. *Mater Charact*, 2017, 132: 53-68.
- [7] CHEN Z, JOHAN M, PENG R L, et al. Surface integrity and fatigue performance of Inconel 718 in wire electrical discharge machining[J]. *Procedia Cirp*, 2016, 45: 307-310.
- [8] YADAV S P, PAWADE R S. Manufacturing methods induced property variations in Ti6Al4V using high-speed machining and additive manufacturing (AM)[J]. *Metals*, 2023, 13(2): 287.
- [9] WUSATOWSKA-SARNEK A M, DUBIEL B, CZYRSKA-FILEMONOWICZ A, et al. Micro-structural characterization of the white etching layer in nickel-based superalloy[J]. *Metallurgical and Materials Transactions A*, 2011, 42(12): 3813-3825.
- [10] HARDY M C, HERBERT C R J, KWONG J, et al. Characterizing the integrity of machined surfaces in a powder nickel alloy used in aircraft engines[C]//Proceedings of the 2nd CIRP Conference on Surface Integrity. [S.l.]:[s.n.], 2014: 411-416.
- [11] HERBERT C R J, AXINTE D A, HARDY M C, et al. Investigation into the characteristics of white layers produced in a nickel-based superalloy from drilling operations[C]//Proceedings of the 1st CIRP Conference on Surface Integrity. [S.l.]:[s.n.], 2011, 19: 138-143.
- [12] BONNARDEL Q, WAGNER V, DESSEIN G, et al. Effects of cutting parameters over turning of UDIMET 720 superalloy in a broaching process simulation[C]//Proceedings of the 16th CIRP Conference on Modelling of Machining Operations. [S.l.]:[s.n.], 2017, 58: 572-577.
- [13] QUAN F, CHEN Z T, YE H, et al. Study of the effect of surface roughness on fatigue strength of GH4169 based on indirect evaluation of the notch root radius[J]. *International Journal of Fatigue*, 2021, 152: 106440.
- [14] XU Y C, GONG Y D, WANG Z X, et al. Experimental study of Ni based single crystal superalloy microstructure evolution and work hardening of ground subsurface[J]. *Archives of Civil and Mechanical Engineering*, 2021, 21: 43.
- [15] HAMID J, WALID J, VICTOR S, et al. Inconel 718 superalloy controlled surface integrity for fatigue applications produced by precision turning[J]. *International Journal of Precision Engineering and Manufacturing*, 2019, 20: 1297-1310.
- [16] KRÄMER A, DIETER L, FRITZ K. High performance cutting of aerospace materials[J]. *Advanced Materials Research*, 2012, 498: 127-132.
- [17] KONG X W, LI B, JIN Z B, et al. Broaching performance of superalloy GH4169 based on FEM[J]. *Mater Sci Technol*, 2011, 27(12): 1178-1184.
- [18] LIANG X L, LIU Z Q, WANG B. State-of-the-art of surface integrity induced by tool wear effects in machining process of titanium and nickel alloys: A review[J]. *Measurement*, 2019, 132: 150-181.
- [19] CANEDA S, AYESTA I, WANG J, et al. Study on the influence of the actual industrial constrains during WEDM roughing of Fir Trees on Inconel® 718 disks[J]. *Procedia CIRP*, 2022, 113: 131-136.
- [20] RENGEND, CRAIG K, LI H Y, et al. Characterization of plastic deformation induced by machining in a Ni-based superalloy[J]. *Materials Science and Engineering A*, 2020, 778: 139104.
- [21] ROBERTO G, FANTERIA D. Influence of turning parameters on the high-temperature fatigue performance of Inconel 718 superalloy[J]. *Fatigue & Fracture of Engineering Materials & Structures*, 2017, 40(12): 2019-2031.
- [22] TELESMAJAN J, GABB T P, KANTZOS P T, et al. Effect of a large population of seeded alumina inclusions on crack initiation and small crack fatigue crack growth in Udimet 720 nickel-base disk[J]. *International Journal of Fatigue*, 2021, 142: 105953.
- [23] DAN G, MIKE G, HARRY K. Manufacturing related residual stresses and turbine disk life prediction[C]//Proceedings of American Institute of Physics Conference. Golden, Colorado, USA: [s.n.], 2005, 760: 1339.
- [24] HUA Y, LIU Z Q. Effects of machining induced residual shear and normal stresses on fatigue life and stress intensity factor of Inconel 718[J]. *Applied Sciences*, 2019, 9(22): 4750.
- [25] HUA Y, LIU Z Q. Experimental investigation of principal residual stress and fatigue performance for turned nickel-based superalloy Inconel 718[J]. *Materials*, 2018, 11(6): 879.
- [26] QUAN F, CHEN Z T, LI Q T, et al. Effects of pro-

cess combinations of milling, grinding, and polishing on the surface integrity and fatigue life of GH4169 components[J]. Proceedings of the Institution of Mechanical Engineers, Part B, Journal of Engineering Manufacture, 2020, 234(3): 538-548.

- [27] CHEN Z, MOVERARE J J, PENG R L, et al. On the conjoint influence of broaching and heat treatment on bending fatigue behavior of Inconel 718[J]. Mater Sci Eng: A, 2016, 671: 158-169.
- [28] TELESMA J, GABB T P, KANTZOS P T, et al. Effect of broaching machining parameters, residual stresses and cold work on fatigue life of Ni-based turbine disk P/M alloy at 650 °C[J]. International Journal of Fatigue, 2021, 150: 106328.
- [29] CONNOLLEY T, STARINK M J, REED P A S. Effect of broaching on high-temperature fatigue behavior in notched specimens of INCONEL 718[J]. Metallurgical and Materials Transactions A, 2004, 35(3): 771-783.
- [30] KIM I S, CHOI B G, JUNG J E, et al. Effect of microstructural characteristics on the low cycle fatigue behaviors of cast Ni-base superalloys[J]. Materials Characterization, 2015, 106: 375-381.
- [31] CHEN X, YANG Z Q, SOKOLOV M A, et al. Low cycle fatigue and creep-fatigue behavior of Ni-based alloy 230 at 850 °C[J]. Materials Science and Engineering: A, 2013, 563: 152-162.
- [32] HE L Z, ZHENG Q, SUN X F, et al. High temperature low cycle fatigue behavior of Ni-base superalloy M963[J]. Materials Science and Engineering: A, 2005, 402(1/2): 33-41.

Acknowledgements This work was supported by the National Natural Science Foundation of China (No. 12250710129), the Natural Science Foundation of Jiangsu

Province (No. BK20200450), the China Postdoctoral Science Foundation (Nos. 2023M731823, 2020TQ0144), and the Fundamental Research Foundation for the Central Universities (No. NS2022019).

Authors Dr. ZHANG Lu received his B.S. degree in Mathematics from Shandong University in 2010 and Ph.D. degree in Solid Mechanics of Advance Materials from Loughborough University, UK, in 2019, respectively. He joined in Nanjing University of Aeronautics and Astronautics in November 2019, where he is a lecturer of College of Energy and Power Engineering. His research is focused on aeroengine structural integrity, constitutive theory and fatigue life prediction of superalloy and composite materials, structural design principle and method of ceramic matrix composite materials, etc.

Prof. SONG Yingdong received the B.E., M.S., and Ph.D. degrees from Nanjing University of Aeronautics and Astronautics. He serves as the chairman of the Composites Society of Jiangsu Province. His research interest mainly focuses on the structural design and integrity assessment of ceramic matrix composites components for aeroengine application, fatigue failure behaviors and life predication of superalloys, etc.

Author contributions Dr. ZHANG Lu designed the study, carried out the experiments and conducted the analysis. Prof. SONG Yingdong and Prof. JIANG Rong contributed to the methods of analysis. Mr. LI Weilong interpreted the results and wrote the manuscript. Mr. YU Zhiwei designed the experiments. Mr. WANG Yuzhuo contributed to the manuscript writing. All authors commented on the manuscript draft and approved the submission.

Competing interests The authors declare no competing interests.

(Production Editor: WANG Jing)

铣削工艺参数对镍基粉末高温合金 650 °C 低周疲劳寿命的影响

张 禄^{1,2}, 李伟龙^{1,2}, 王玉卓^{1,2}, 余志伟^{1,2}, 江 荣^{1,2}, 宋迎东^{1,2,3}

(1. 南京航空航天大学能源与动力学院, 工业和信息化部航空发动机热环境与热结构重点实验室, 南京 210016, 中国; 2. 南京航空航天大学能源与动力学院, 江苏省航空动力系统重点实验室, 南京 210016, 中国; 3. 南京航空航天大学机械结构力学及控制国家重点实验室, 南京 210016, 中国)

摘要: 研究了不同铣削工艺对疲劳损伤的影响规律。对采用 4 种工艺加工的试样进行了 650 °C 高温空气环境下的低周疲劳试验。分别采用粗糙度表征方法、背向散射电子衍射技术和纳米压痕测试以获得试样的表面粗糙度、残余应力和加工硬化。测试结果表明, 采用电火花线切割方法加工的试样疲劳寿命最高(平均 80 360 循环), 有最低的表面粗糙度(0.226)和残余应力; 而钝刀具加工的试样疲劳寿命最低(平均 43 978 循环), 相较于电火花线切割试样的疲劳寿命下降了 45%。扫描电镜表征结果表明, 疲劳裂纹主要由粗大的非再结晶晶粒和加工缺陷引发。铣削加工方法和参数对疲劳损伤程度和疲劳寿命有重要影响。

关键词: 铣削工艺; 疲劳寿命; 镍基粉末高温合金; 表面粗糙度; 残余应力; 加工硬化